

We are IntechOpen, the world's leading publisher of Open Access books Built by scientists, for scientists

6,900

Open access books available

185,000

International authors and editors

200M

Downloads

Our authors are among the

154

Countries delivered to

TOP 1%

most cited scientists

12.2%

Contributors from top 500 universities



WEB OF SCIENCE™

Selection of our books indexed in the Book Citation Index
in Web of Science™ Core Collection (BKCI)

Interested in publishing with us?
Contact book.department@intechopen.com

Numbers displayed above are based on latest data collected.
For more information visit www.intechopen.com



Origin and Fundamentals of Perovskite Solar Cells

Mohd Quasim Khan and Khursheed Ahmad

Abstract

In the last few decades, the energy demand has been increased dramatically. Different forms of energy have utilized to fulfill the energy requirements. Solar energy has been proven an effective and highly efficient energy source which has the potential to fulfill the energy requirements in the future. Previously, various kind of solar cells have been developed. In 2013, organic–inorganic metal halide perovskite materials have emerged as a rising star in the field of photovoltaics. The methyl ammonium lead halide perovskite structures were employed as visible light sensitizer for the development of highly efficient perovskite solar cells (PSCs). In 2018, the highest power conversion efficiency of 23.7% was achieved for methyl ammonium lead halide based PSCs. This obtained highest power conversion efficiency makes them superior over other solar cells. The PSCs can be employed for practical uses, if their long term stability improved by utilizing some novel strategies. In this chapter, we have discussed the optoelectronic properties of the perovskite materials, construction of PSCs and recent advances in the electron transport layers for the fabrication of PSCs.

Keywords: methyl ammonium lead halide, perovskites light absorbers, photovoltaics, perovskite solar cells

1. Introduction

The researchers believe that the solar energy have the potential to fulfill the energy requirements [1]. The earth receive enormous amount of solar energy in the form of sunlight [2]. This sunlight can be converted to the electrical energy to fulfill our energy requirements [3]. The photovoltaic device (solar cells) can directly converted the sunlight to the electricity [4]. In previous decades, different kinds of photovoltaic devices (dye-sensitized solar cells = DSSCs, organic solar cells = OSCs, polymer solar cells, quantum-dot sensitized solar cells and perovskite solar cells) were developed [5–9]. These kinds of solar cells have attracted the scientific community due to their simple manufacturing procedure and cost-effectiveness [10].

The PSCs gained huge attention because of their excellent photovoltaic performance and low-cost [11–16]. The perovskite solar cells (PSCs) involve a perovskite light absorber layer. The perovskite is a material which has a molecular formula of ABO_3 . The perovskite term was given to the calcium titanate ($CaTiO_3$). There is also another class of perovskite materials exists with molecular formula of ABX_3 (where $A = Cs^+$, $CH_3NH_3^+$; $B = Pb^{2+}$ or Sn^{2+} and $X = I^-$, Br^- or Cl^-). This class of perovskite materials possesses excellent absorption properties, charge carrier properties and suitable band gap. In 2009, Kojima et al. [17] prepared the methyl ammonium lead

halide (MAPbX_3 ; where $\text{MA} = \text{CH}_3\text{NH}_3^+$, $\text{X} = \text{halide anion}$) perovskite materials and investigated their optoelectronic properties. Further, authors fabricated the dye sensitized solar cells using MAPbX_3 visible light sensitizer [17]. The performance of the developed dye sensitized solar cells was evaluated and the device exhibited good power conversion efficiency (PCE) and open circuit voltage. The fabricated dye sensitized solar cells with MAPbX_3 visible light sensitizer exhibited the good PCE of $\sim 3.8\%$ [17]. Although, this power conversion efficiency was quite interesting but the presence of liquid electrolyte vanished this performance. Hence, it was observed that the use of alternative solid state electrolyte/hole transport material would be of great significance. In this regard, numerous strategies were developed to overcome the issue of liquid electrolyte. In this regard, a solid state electrolyte was employed by Lee et al. [18] to develop the PSCs. The developed PSCs device showed the good power conversion efficiency of 10.9% . In last few years, various novel approaches were advanced to improve the photovoltaic performance of the PSCs [19–30] and recently the best PCE of 23.3% was achieved for PSCs [31].

In this chapter, we have discussed the construction of PSCs. Recent advances in PSCs with respect to the charge collection layer/electron transport layer and future prospective have also been discussed.

2. Construction of PSCs

The fabrication of PSCs required different layers such as transparent conductive oxide coated fluorine doped tin oxide = FTO, electron transport layer (generally consists of semiconducting metal oxides), light absorber layer (perovskite), hole transport material (HTM) layer and metal contact (Au) layer. In the first step, FTO glass substrate etched with the help of zinc powder and HCl followed by the washing of the etched FTO glass substrate with acetone, DI water and 2-propanol. The compact layer of the TiO_2 deposited on to the FTO glass substrate using spin coater and annealed at $\sim 500^\circ\text{C}$ for 30–40 min. Further electron transport layer also deposited on the electrode using spin coater and annealed at $\sim 500^\circ\text{C}$ for 30–40 min. The perovskite light absorber layer deposited using spin coater and annealed at $\sim 80\text{--}120^\circ\text{C}$ for 20–60 min. Further, hole transport material (HTM) also deposited using spin coater. Finally the metal contact layer (Au) deposited using thermal evaporation approach. The construction of PSCs has been presented in **Figure 1**.

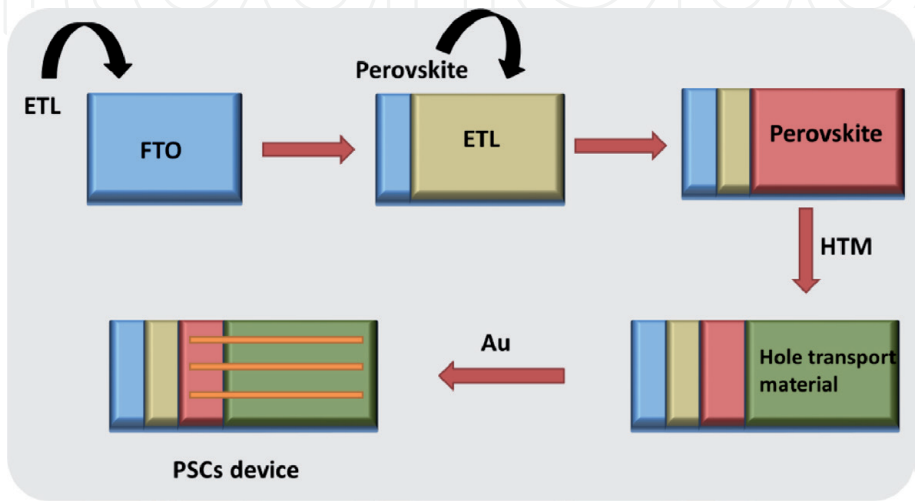


Figure 1.
Fabrication process for the PSCs.

The photovoltaic performance of the constructed PSCs can be determined by different techniques like external quantum efficiency (EQE), photocurrent-voltage (I-V), photoluminescence spectroscopy and incident-photo-to-current-conversion efficiency = IPCE etc. In general, the performance of any solar cell device can be determined in terms of fill factor, PCE, photocurrent density and open circuit voltage. Photoluminescence spectroscopy can also be employed to check the lifetime of the generated electrons inside the perovskite materials which is related to the recombination processes. It has also been known that the PSCs devices with high electron lifetime and lower recombination reaction rates may provide better photovoltaic performance in terms of power conversion efficiency.

The PSCs device absorbs the sunlight which created the electron-hole pairs inside the perovskite light absorber layer. This electron has to be transferred to the conductive electrode surface. Thus, electron transport layer consists of transition metal oxides (generally TiO_2 or SnO_2) transport this generated electron to the conductive electrode (FTO). The hole can be collected by the hole transport material layers. In some cases, the transferred electron can recombine and influence the performance of the PSCs device. Thus, some buffer or compact layers have been used to reduce the recombination process. The perovskite materials used in such PSCs devices worked as light absorber.

3. Origin of PSCs

The PSCs were originated in 2009 by Kojima et al. [17] and reported an interesting PCE of 3.1%. Further different approaches were utilized to improve the PCE of the PSCs. Recently, Tang et al. [32] prepared the low temperature processed zinc oxide nanowalls (ZnO NWs). Authors employed these prepared ZnO NWs as electron collection layer for the development of PSCs [32]. The morphological features of the prepared ZnO NWs were determined by scanning electron microscopy = SEM and transmission electron microscopy = TEM. The SEM and TEM results confirmed the formation of ZnO NWs. Further PSCs were constructed using ZnO NWs as electron collection layer whereas MAPbI_3 as light absorber. The device architecture of the PSCs has been presented in **Figure 2a**. The energy level values of the perovskite light absorber, ZnO, indium doped tin oxide (ITO), spiro-OMeTAD and Ag have been displayed in **Figure 2b**.

The performance of the PSCs devices with ZnO NWs and ZnO thin films were evaluated by J-V analysis. The J-V curves of the PSCs developed with ZnO NWs and ZnO thin films have been depicted in **Figure 2c**. The constructed PSCs device with ZnO NWs exhibited the highest PCE of 13.6% whereas the PSCs developed with ZnO thin films showed the PCE of 11.3%. This showed that ZnO NWs plays crucial role in charge collection compare to the ZnO thin films. The NWs of ZnO collect the generated electron more efficiently compare to the ZnO thin films. Further, incident IPCE of the constructed PSCs was also checked. The IPCE curves of the PSCs developed with ZnO NWs and ZnO thin films have been presented in **Figure 2d**. The PSCs developed with ZnO NWs showed the highest open circuit voltage of 1000 mV whereas the PSCs device fabricated with ZnO thin films showed the open circuit voltage of 980 mV. The constructed PSCs with ZnO NWs exhibited the improved IPCE compared to the PSCs device developed with ZnO thin films.

In other work, Mahmud et al. [33] synthesized low-temperature processed ZnO thin film.

The optical properties of the prepared ZnO thin film were investigated by employing ultraviolet-visible (UV-vis) absorption spectroscopy. The Tauc plot of the ZnO has been presented in **Figure 3A**. The synthesized ZnO possess an optical band gap of

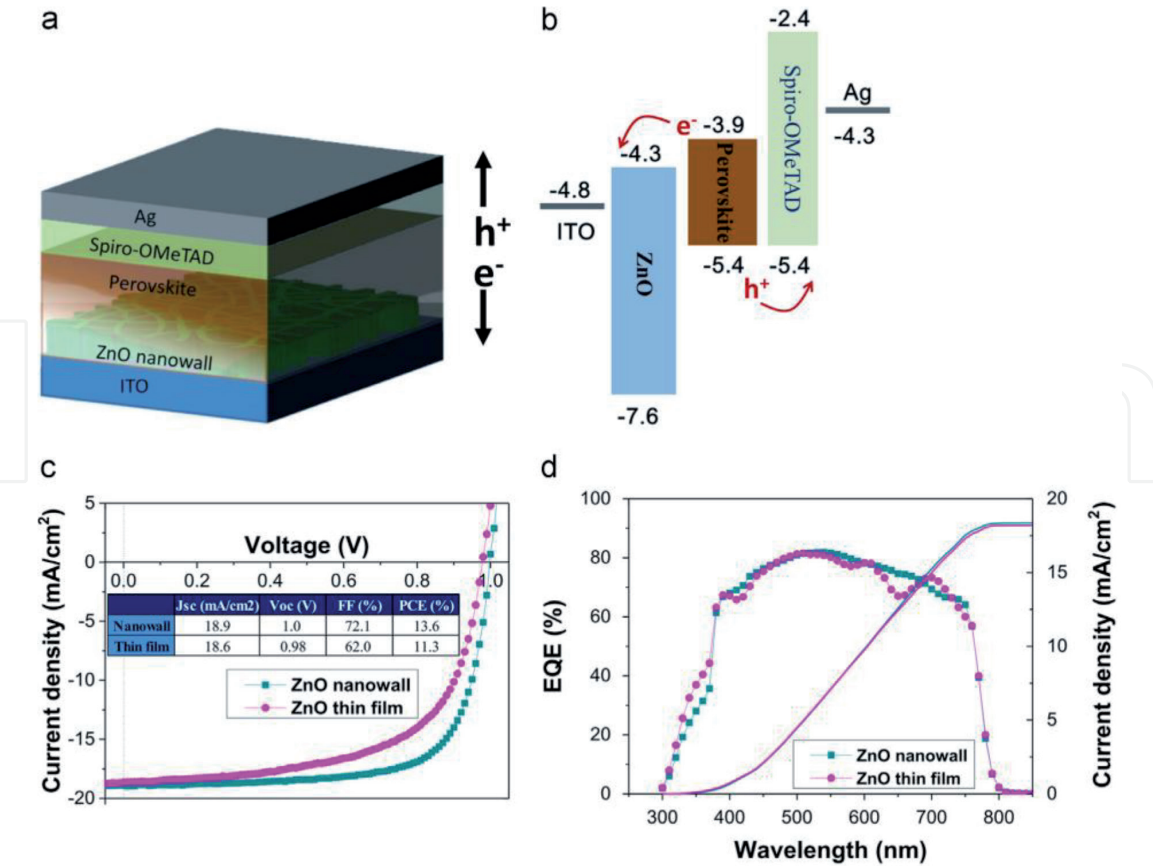


Figure 2. Schematic picture of PSCs device architecture (a). Energy level diagram of PSCs components (b). J-V graphs of the PSCs constructed with ZnO NWs and ZnO thin films (c). IPCE of the PSCs constructed with ZnO NWs and ZnO thin films (d). Reprinted with permission [32].

3.53 eV as confirmed by Tauc relation. The formation of ZnO on ITO glass substrate was confirmed by employing X-ray diffraction = XRD method. The XRD pattern of the ZnO has been presented in **Figure 3B**. The XRD pattern of the ZnO showed the crystalline nature with strong diffraction peaks. Authors employed ZnO thin film as electro transport layer for the construction of PSCs [33]. The MAPbI_3 was utilized as light absorber layer. Authors also investigated the morphological features of the MAPbI_3 films prepared on ZnO. The SEM results showed the presence of uniform surface morphology of the MAPbI_3 perovskite [33]. Further, PSCs were fabricated and the device architecture of the fabricated PSCs has been depicted in **Figure 4A**.

The energy level diagram of the fabricated PSCs device has been presented in **Figure 4B**. The photovoltaic performance of the constructed PSCs device was evaluated by recording J-V curve. The obtained results showed that the fabricated PSCs device with ZnO thin film possess a highest PCE of 8.77% with open circuit voltage of 932 mV.

In 2017, Li et al. [34] synthesized $\text{ZnO}/\text{Zn}_2\text{SnO}_4$ under facile conditions. The synthesized $\text{ZnO}/\text{Zn}_2\text{SnO}_4$ was utilized as compact layer for the fabrication of MAPbI_3 based PSCs. Authors recorded the XRD pattern of the MAPbI_3 perovskite layer [34]. The XRD pattern of the MAPbI_3 perovskite layer has been presented in **Figure 5a**.

The XRD pattern of the MAPbI_3 perovskite layer showed the well-defined diffraction planes which suggested the successful formation of MAPbI_3 perovskite as shown in **Figure 5a**. The formation of the $\text{ZnO}/\text{Zn}_2\text{SnO}_4$ was checked by XRD and X-ray photoelectron spectroscopy (XPS). The recorded XRD pattern of the $\text{ZnO}/\text{Zn}_2\text{SnO}_4$ has been presented in **Figure 5b**. The XRD pattern showed the diffraction planes for the ZnO, Zn_2SnO_4 and SnO_2 .

This confirmed the formation of $\text{ZnO}/\text{Zn}_2\text{SnO}_4$. Further, authors also investigated the morphological characteristics of the $\text{ZnO}/\text{Zn}_2\text{SnO}_4$ using SEM analysis

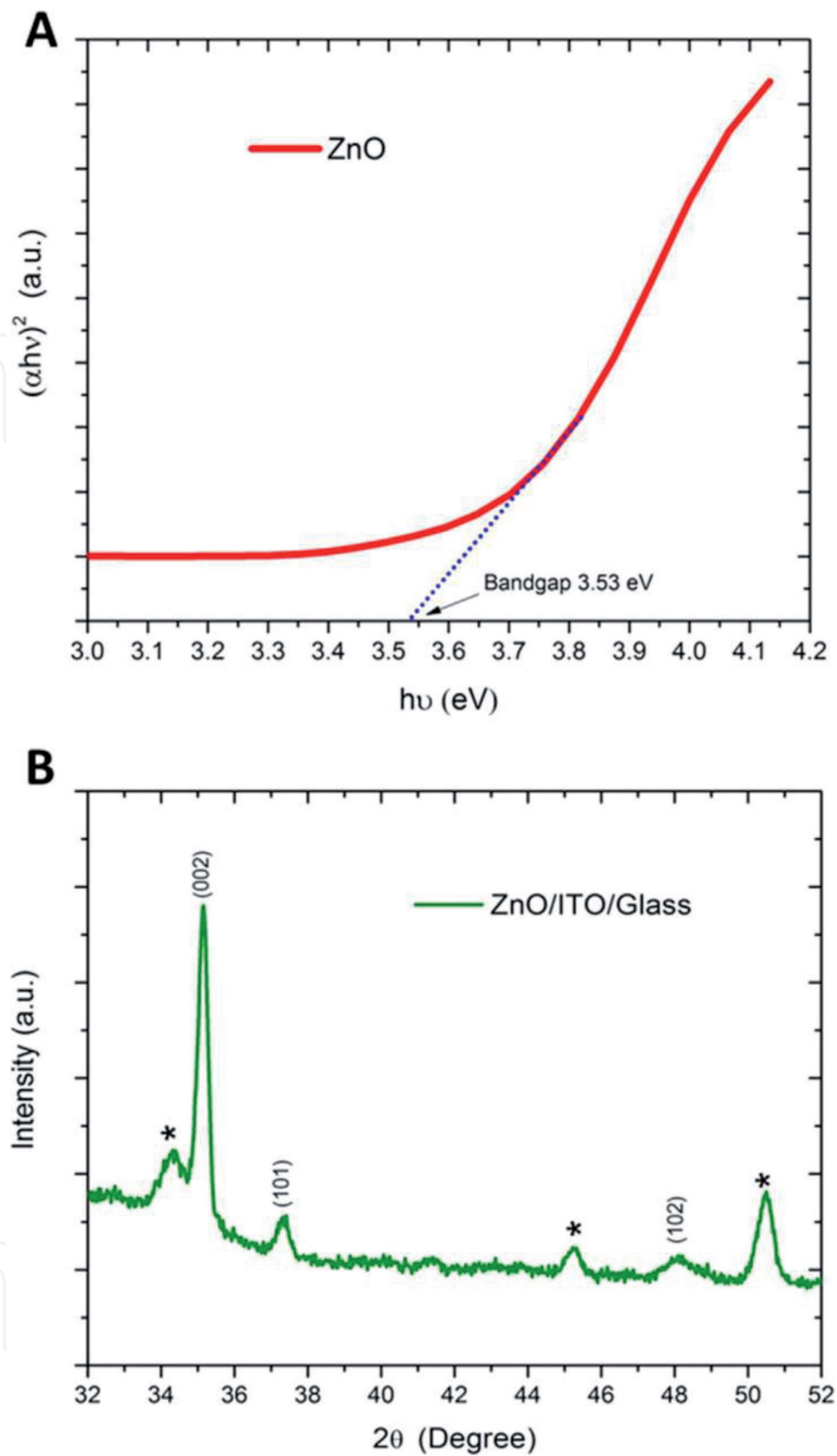


Figure 3.
Tauc plot of the ZnO (A). XRD pattern of the ZnO/ITO (B). Reprinted with permission [33].

[34]. Authors employed ZnO/Zn₂SnO₄ as compact layer and developed the PSCs devices [34]. Authors also developed the PSCs using TiO₂ with different thickness [34]. The performance of the developed PSCs devices were evaluated by J-V approach. The recorded J-V curves of the developed PSCs with different thicknesses (40 nm, 60 nm, 80 nm, 100 nm and 120 nm) of TiO₂ have been presented in **Figure 6**. The PSCs device fabricated with TiO₂ (thickness = 100 nm) exhibited the highest performance compared to the PSCs device fabricated with TiO₂ of different thicknesses.

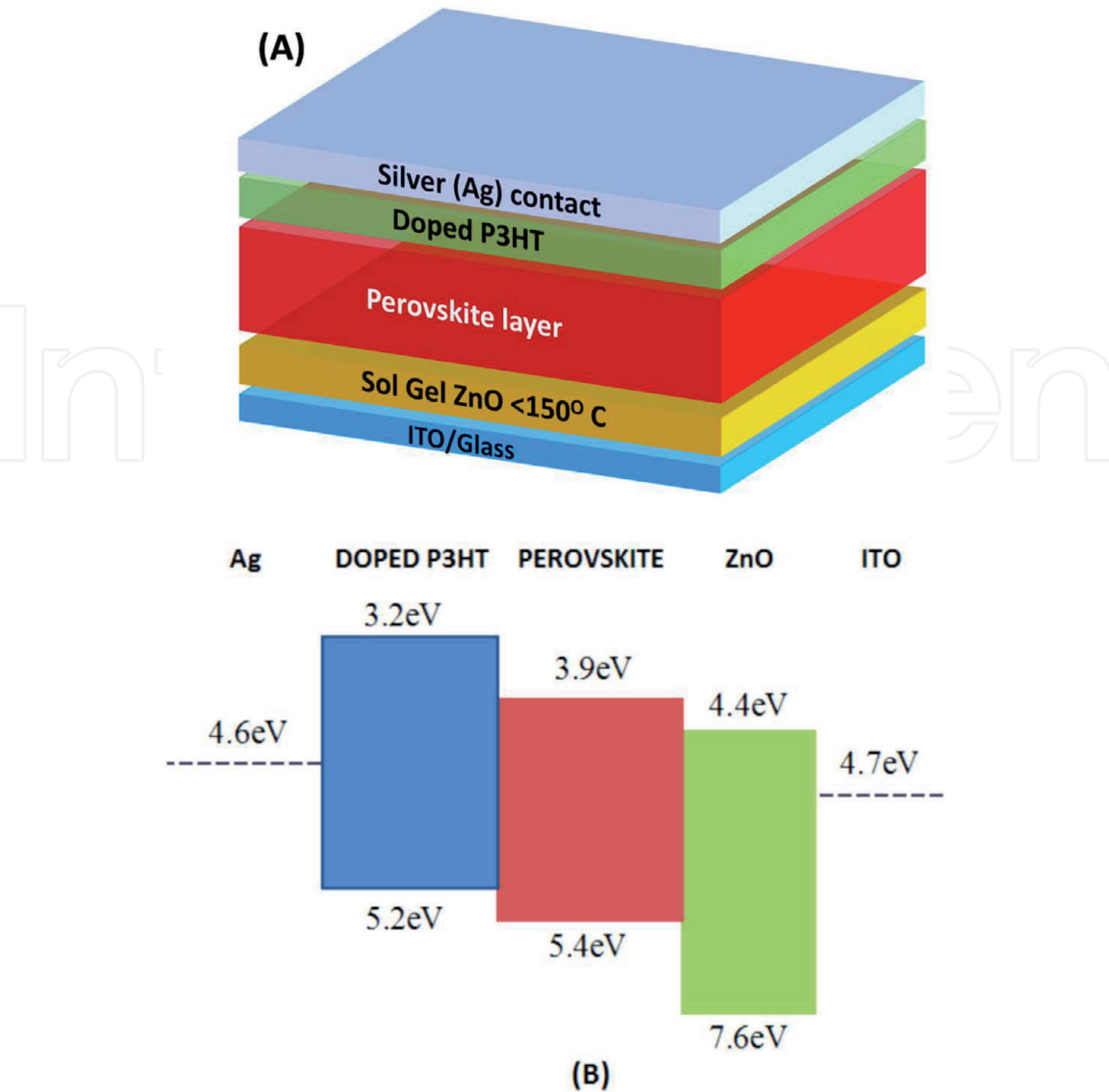


Figure 4. Schematic diagram of the PSCs device (A). Energy level diagram of the PSCs (B). Reprinted with permission [33].

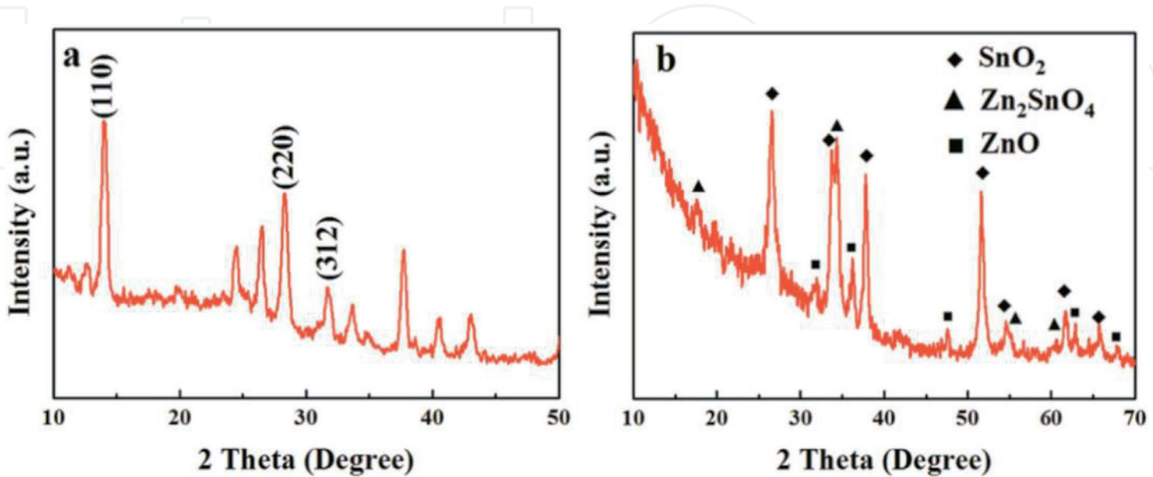


Figure 5. XRD patterns of the MAPbI₃ (a) and ZnO/ZSO CL (b). Reprinted with permission [34].

Furthermore, the photovoltaic performance of the PSCs developed using ZnO/ Zn₂SnO₄ as compact layer with different thickness (15 nm, 35 nm, 55 nm, 75 nm and 95 nm) were also evaluated. The J-V curves of the PSCs developed using ZnO/

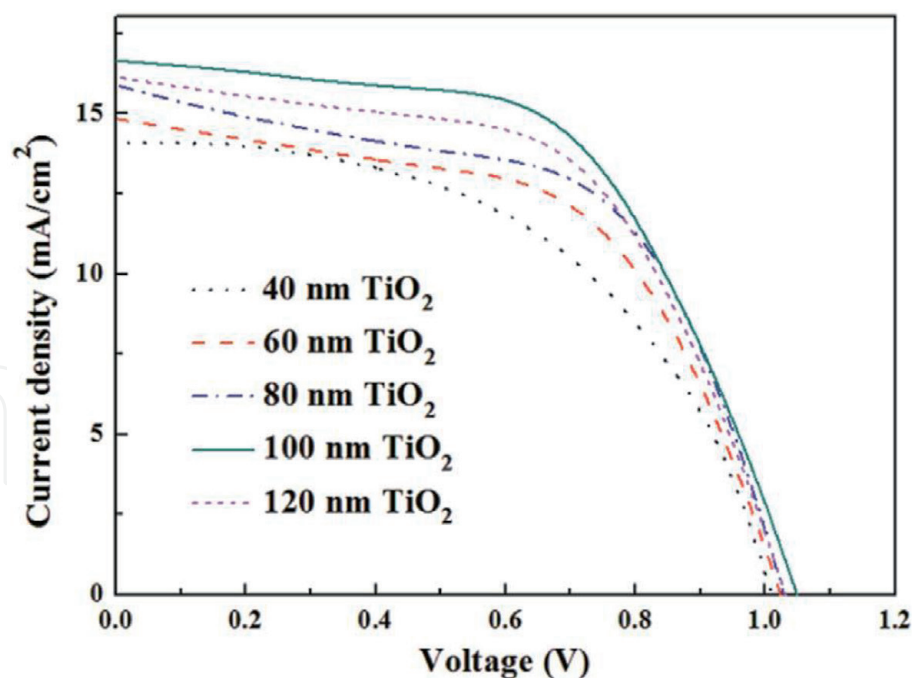


Figure 6.
J-V curves of PSCs based on different thickness of TiO₂ CLs. Reprinted with permission [34].

Zn₂SnO₄ with different thickness (15 nm, 35 nm, 55 nm, 75 nm and 95 nm) has been presented in **Figure 7**. Authors found that the PSCs device fabricated with ZnO/Zn₂SnO₄ (thickness = 15 nm) has poor photovoltaic parameters which resulted to the poor performance [34].

The PSCs device fabricated with ZnO/Zn₂SnO₄ (thickness = 75 nm) showed enhanced photovoltaic parameters which resulted to the improved photovoltaic performance (**Figure 7**). This showed that ZnO/Zn₂SnO₄ (thickness = 75 nm) is more effective charge compact layer compared to the TiO₂.

In another recent work, Chang et al. [35] developed the PSCs using Ce doped CH₃NH₃PbI₃ perovskite light absorber layer.

In this work, Chang et al. [35] prepared the thin films of Ce doped CH₃NH₃PbI₃ perovskite light absorber layer using a post treatment approach. Authors used CsI to promote the morphological features and crystallization of the thin films of Ce doped CH₃NH₃PbI₃ perovskite light absorber layer. The use of Cs helps to obtain the large grain size of the CH₃NH₃PbI₃ perovskite. The grain size of the CH₃NH₃PbI₃ perovskite absorber layers were ranges 270 nm–650 nm. The formation of the perovskite light absorber layers were confirmed by XRD analysis. The optical band gap of the perovskite light absorber layer was also calculated by using Tauc relation.

The Cs doped CH₃NH₃PbI₃ perovskite light absorber has a band gap of 1.59 eV whereas this band gap slightly increases with increasing CsI concentrations. The increase in the optical band gap of the CH₃NH₃PbI₃ perovskite absorber layer also confirmed the insertion of Cs in to the perovskite light absorber layer.

The SEM pictures of the CH₃NH₃PbI₃ perovskite light absorber layers were also recorded. The recorded SEM pictures of the CH₃NH₃PbI₃ perovskite light absorber layers without and with CsI treatment have been presented in **Figure 8a–f**. The SEM picture of the CH₃NH₃PbI₃ perovskite light absorber layer without CsI treatment showed the small grain size (**Figure 8a**). However, the insertion of CsI to the CH₃NH₃PbI₃ perovskite light absorber layer increases the grain size as confirmed by the SEM investigations. The highly uniform surface morphology was observed in case of CH₃NH₃PbI₃ perovskite absorber layer treated with 6mg mL⁻¹ CsI (**Figure 8d**). Furthermore, PSCs devices were fabricated using CH₃NH₃PbI₃ perovskite light absorber layers. The schematic picture of the developed PSCs device has been presented in **Figure 9**. The

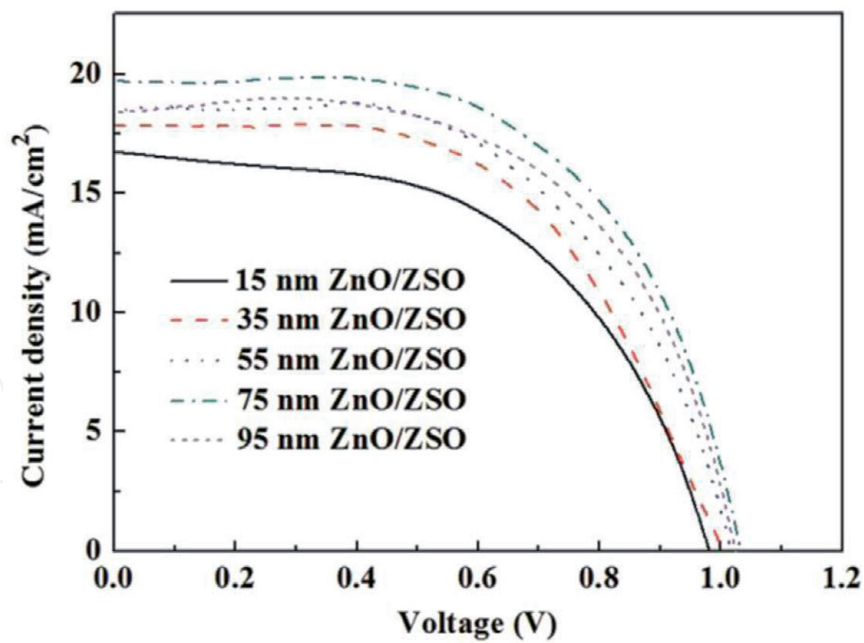


Figure 7. *J-V curves of PSCs based on different thickness of ZnO/ZSO CLs. Reprinted with permission [34].*

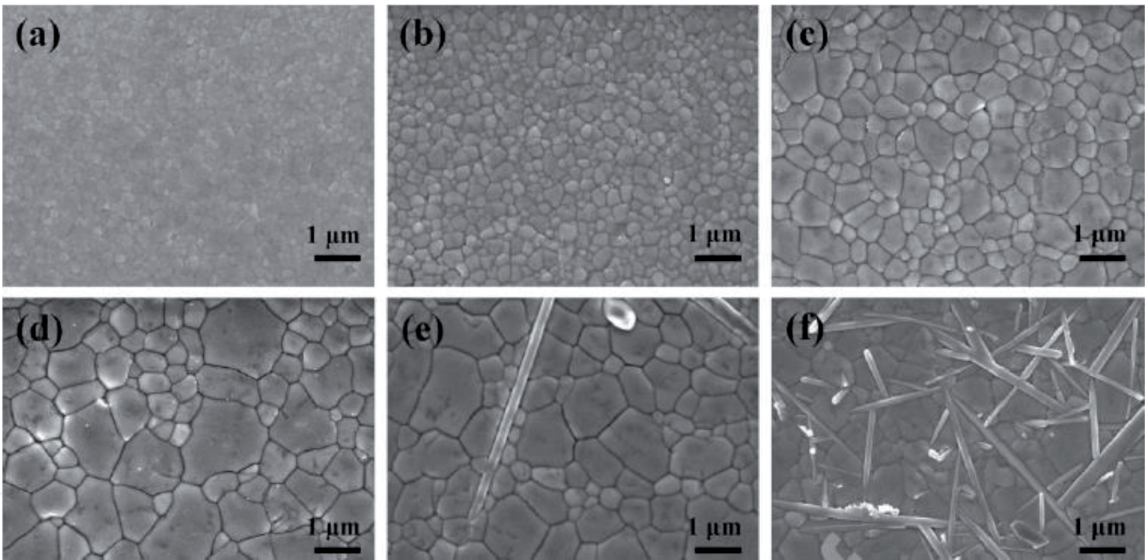


Figure 8. *SEM pictures of the CH₃NH₃PbI₃ thin films: untreated (a) and treated with 2.5 mg mL⁻¹ (b), 5 mg mL⁻¹ (c), 6 mg mL⁻¹ (d), 7 mg mL⁻¹ (e), 9 mg mL⁻¹ CsI (f). Reprinted with permission [35].*

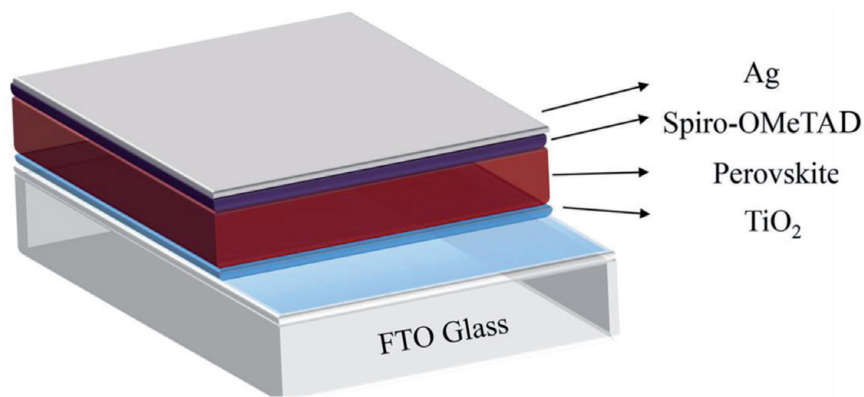


Figure 9. *Schematic picture of the constructed PSCs device. Reprinted with permission [35].*

Absorber layer	J _{SC} (mA/cm ²)	V _{OC} (mV)	PCE (%)	Type of solar cells	References
MAPbI ₃	19.2	720	10.2	PSCs	[36]
perovskite	22.7	240	2.02	PSCs	[37]
MASnI ₃	16.8	880	6.4	PSCs	[38]
FASnI ₃	17.53	600	6.7	PSCs	[39]
FASnI ₃	24.1	520	9	PSCs	[40]
MASnI ₃	11.1	970	7.6	PSCs	[41]
FASn _{0.5} Pb _{0.5} I ₃	21.9	700	10.2	PSCs	[42]
MASn _{0.25} Pb _{0.75} I ₃	15.8	730	7.37	PSCs	[43]
Al ³⁺ doped CH ₃ NH ₃ PbI ₃	22.4	1001	19.1	PSCs	[44]
Dye	13.2	570	4.63	DSSCs	[45]
Dye	15.46	821	8.20	DSSCs	[46]
Polymer light absorber	20.65	946	14.45	Polymer	[47]
Polymer light absorber	19.1	990	11.5	Polymer	[48]
Perovskite quantum dot	15.1	1220	13.8	Quantum dot PSCs	[49]
Quantum dot light absorber	26.70	780	13.84	Quantum dot solar cells	[50]
Organic light absorbing material	21.8	940	14.8	Organic solar cells	[51]

Table 1.
Comparison of the photovoltaic parameters of the PSCs with other reported solar cells.

constructed PSCs device with CH₃NH₃PbI₃ perovskite absorber layer (with 6 mg mL⁻¹ CsI treatment) exhibited the best PCE of 14.4% with open circuit voltage of 1.05 V. However, the PSCs developed without CsI treatment showed the relatively lower PCE of 10.5%. There are different kinds of solar cells existed and each type of solar cell has different light absorbing materials. The photovoltaic performance of the PSCs has been compared with other reported solar cells as shown in **Table 1**.

4. Future prospective

Since the origin, PSCs have received enormous attention due to their simple solution-processed fabrication, high performance and cost-effectiveness. This is because of the excellent optoelectronic properties of the organic–inorganic lead halide perovskite light absorbers. The PSCs achieved a highest power conversion efficiency of more than 24%. The PSCs can be employed for practical applications due to their high performance and cost-effectiveness. However, the poor aerobic stability and moisture sensitivity of the perovskite light absorbers restricts their practical applications. Thus, it is of great importance to overcome the issue of moisture sensitivity and poor stability of the PSCs. In previous years numerous strategies and methods were developed to enhance the stability of the PSCs. However, further improvements are necessary to commercialize the PSCs at large scale.

We believe that the following points/strategies would be beneficial to further enhance the stability and photovoltaic performance of the PSCs:

1. New device architectures are required to develop the highly efficient PSCs.
2. The photovoltaic parameters/performance of the PSCs can be further improved by utilizing/developing new electron transport/charge extraction layers.

3. Some novel hydrophobic cationic groups should be introduced to the perovskite light absorbers to improve the aerobic stability and moisture sensitivity.

5. Conclusions

In present scenario, energy crisis is the major challenge for today's world. Solar cells have the potential to overcome the issue of energy crisis. In last 10 years, PSCs have attracted the materials scientists due to its excellent photovoltaic performance and easy fabrication procedures. The highly efficient PSCs involve MAPbX₃ as light absorber layer. The photovoltaic performance of the PSCs can be influenced by the presence of absorber layer or electron transport layer. Previously different kinds of electron transport layers have been widely studied to enhance the performance of the MAPbX₃ based PSCs. The highest PCE of more than 24% has been certified by NREL for MAPbX₃ based PSCs device. This excellent PCE is close to the commercialized silicon based solar cells. Thus, it can be said that PSCs can fulfill our energy requirements in the future. In this chapter, the fabrication of PSCs has been discussed. The recent advances in the development of PSCs with different compact layers, electron transport layers and charge collection layers have been reviewed.

Acknowledgements

K.A. would like to acknowledge Discipline of Chemistry, IIT Indore. M.Q.K. acknowledged Department of Chemistry, Faculty of Applied Science and Humanities, Invertis University.

Conflict of interest

"The authors declare no conflict of interest."

Author details


Mohd Quasim Khan¹ and Khursheed Ahmad^{2*}

¹ Department of Chemistry, Faculty of Applied Science and Humanities, Invertis University, Bareilly, 243123, U.P., India

² Discipline of Chemistry, Indian Institute of Technology Indore, Simrol, Khandwa Road, 453552, M.P., India

*Address all correspondence to: khursheed.energy@gmail.com

IntechOpen

© 2020 The Author(s). Licensee IntechOpen. This chapter is distributed under the terms of the Creative Commons Attribution License (<http://creativecommons.org/licenses/by/3.0>), which permits unrestricted use, distribution, and reproduction in any medium, provided the original work is properly cited. 

References

- [1] Reddy VS, Kaushik SC, Ranjan KR, Tyagi SK. State-of-the-art of solar thermal power plants. *Renewable and Sustainable Energy Reviews*. 2019;**27**:258-273
- [2] Chen GY, Seo J, Yang CH, Prasad PN. Nanochemistry and nanomaterials for photovoltaics. *Chemical Society Reviews*. 2013;**42**:8304-8338
- [3] Motlak M, Hamza AM, Hammed MG, Barakat NAM. Cd-doped TiO₂ nanofibers as effective working electrode for the dye sensitized solar cells. *Materials Letters*. 2019;**246**:206-209
- [4] O'Regan B, Grätzel M. A low cost, high-efficiency solar cell based on dye-sensitized colloidal TiO₂ films. *Nature*. 1991;**353**:737-740
- [5] Colombo A, Dragonetti C, Roberto D, Ugo R, Manfredi N, Manca P, et al. A carbon doped anatase TiO₂ as a promising semiconducting layer in Ru-dyes based dye-sensitized solar cells. *Inorganica Chimica Acta*. 2019;**489**:263-268
- [6] Zhang X, Liu F, Huang QL, Zhou G, Wang Z-S. Dye-sensitized W-doped TiO₂ solar cells with a tunable conduction band and suppressed charge recombination. *Journal of Physical Chemistry C*. 2011;**115**:12665-12671
- [7] Lu WH, Chou C-S, Chen C-Y, Wu P. Preparation of Zr-doped mesoporous TiO₂ particles and their applications in the novel working electrode of a dye-sensitized solar cell. *Advanced Powder Technology*. 2017;**28**:2186-2197
- [8] Xiang P, Lv F, Xiao T, Jiang L, Tan X, Shu T. Improved performance of quasi-solid-state dye-sensitized solar cells based on iodine-doped TiO₂ spheres photoanodes. *J. Alloy Compound*. 2018;**741**:1142-1147
- [9] Tran VA, Truong TT, Phan TAP, Nguyen TN, Huynh TV, Agrestic A, et al. Application of nitrogen-doped TiO₂ nano-tubes in dye-sensitized solar cells. *Applied Surface Science*. 2017;**399**:515-522
- [10] Deng J, Wang M, Fang J, Song X, Yang Z, Yuan Z. Synthesis of Zn-doped TiO₂ nano-particles using metal Ti and Zn as raw materials and application in quantum dot sensitized solar cells. *J. Alloy Compound*. 2019;**791**:371-379
- [11] Ahmad K, Ansari SN, Natarajan K, Mobin SM. A two-step modified deposition method based (CH₃NH₃)₃Bi₂I₉ perovskite: Lead free, highly stable and enhanced photovoltaic performance. *ChemElectroChem*. 2019;**6**:1192-1198
- [12] Ahmad K, Ansari SN, Natarajan K, Mobin SM. Design and synthesis of 1D-polymeric chain based [(CH₃NH₃)₃Bi₂Cl₉]_n perovskite: A new light absorber material for lead free perovskite solar cells. *ACS Applied Energy Materials*. 2018;**01**:2405-2409
- [13] Ahmad K, Mobin SM. Graphene oxide based planar heterojunction perovskite solar cell under ambient condition. *New Journal of Chemistry*. 2017;**41**:14253-14258
- [14] Ahmad K, Mohammad A, Mobin SM. Hydrothermally grown α-MnO₂ nanorods as highly efficient low cost counter-electrode material for dye-sensitized solar cells and electrochemical sensing applications. *Electrochimica Acta*. 2017;**252**:549-557
- [15] Zhong M, Liang Y, Zhang J, Wei Z, Li Q, Xu D. Highly efficient flexible MAPbI₃ solar cells with a fullerene derivative-modified SnO₂ layer as the electron transport layer. *Journal of Materials Chemistry A*. 2019;**7**:6659-6664

- [16] Guo Z, Ligu G, Zhang C, Xu Z, Ma T. Low-temperature processed non-TiO₂ electron selective layers for perovskite solar cells. *Journal of Materials Chemistry A*. 2018;**6**:4572-4589
- [17] Kojima A, Teshima K, Shirai Y, Miyasaka T. Organometal halide perovskites as visible-light sensitizers for photovoltaic cells. *Journal of the American Chemical Society*. 2009;**131**:6050-6051
- [18] Lee MM, Teuscher J, Miyasaka T, Murakami TN, Snaith HJ. Efficient hybrid solar cells based on meso-superstructured organometal halide perovskites. *Science*. 2012;**338**:643-647
- [19] Chen Y-Z, Wu R-J, Lin LY, Chang WC. Novel synthesis of popcorn-like TiO₂ light scatterers using a facile solution method for efficient dye-sensitized solar cells. *Journal of Power Sources*. 2019;**413**:384-390
- [20] Im JH, Lee CR, Lee JW, Park SW, Park NG. 6.5% efficient perovskite quantum-dot-sensitized solar cell. *Nanoscale*. 2011;**3**:4088-4093
- [21] Kim HS, Lee CR, Im JH, Lee KB, Moehl T, Marchioro A, et al. Lead iodide perovskite sensitized all-solid-state submicron thin film mesoscopic solar cell with efficiency exceeding 9%. *Scientific Reports*. 2012;**2**:591
- [22] Wehrenfennig C, Liu M, Snaith HJ, Johnston MB, Herz LM. Charge-carrier dynamics in vapour-deposited films of the organolead halide perovskite CH₃NH₃PbI₃-xCl_x. *Energy & Environmental Science*. 2014;**7**:2269-2275
- [23] Ma J, Guo X, Zhou L, Lin Z, Zhang C, Yang Z, et al. Enhanced planar perovskite solar cell performance via contact passivation of TiO₂/perovskite interface with NaCl doping approach. *ACS Appl. Energy Mater*. 2018;**1**:3826-3834
- [24] Ke W, Fang G, Wang J, Qin P, Tao H, Lei H, et al. Perovskite solar cell with an efficient TiO₂ compact film. *ACS Applied Materials & Interfaces*. 2014;**6**:15959-15965
- [25] Peng G, Wu J, Wu S, Xu X, Ellis JE, Xu G, et al. Perovskite solar cells based on bottom-fused TiO₂ nanocones. *Journal of Materials Chemistry A*. 2016;**4**:1520-1530
- [26] Lv M, Lv W, Fang X, Sun P, Lin B, Zhang S, et al. Performance enhancement of perovskite solar cells with a modified TiO₂ electron transport layer using Zn-based additives. *RSC Advances*. 2016;**6**:35044-35050
- [27] Liu D, Kelly TL. Perovskite solar cells with a planar heterojunction structure prepared using room-temperature solution processing techniques. *Nat. Photon*. 2014;**8**:133-138
- [28] Jeong S, Seo S, Park H, Shin H. Atomic layer deposition of a SnO₂ electron-transporting layer for planar perovskite solar cells with a power conversion efficiency of 18.3%. *Chemical Communications*. 2019;**55**:2433-2436
- [29] Wang S, Zhu Y, Liu B, Wang C, Ma R. Introduction of carbon nanodots into SnO₂ electron transport layer for efficient and UV stable planar perovskite solar cells. *Journal of Materials Chemistry*. 2019;**7**:5353-5362
- [30] Ding B, Huang SY, Chu QQ, Li Y, Li CX, Li CJ, et al. Low-temperature SnO₂-modified TiO₂ yields record efficiency for normal planar perovskite solar modules. *Journal of Materials Chemistry A*. 2018;**6**:10233-10242
- [31] Zimmermann I, Aghazad S, Nazeeruddin MK. *Angewandte Chemie, International Edition*. 2018;**57**:1-6
- [32] Tang J-F, Tseng Z-L, Chen L-C, Chu S-Y. ZnO nanowalls grown at low-temperature for electron collection

in high-efficiency perovskite solar cells. *Sol. Energ. Mater. Sol. Cells.* 2016;**154**:18-22

[33] Mahmud MA, Kumar N, et al. Low temperature processed ZnO thin film as electron transport layer for efficient perovskite solar cells. *Sol. Energ. Mater. Sol. Cells.* 2017;**159**:251-264

[34] Li W, Jiang Q, Yang J, Luo Y, Li X, Hou Y, et al. Improvement of photovoltaic performance of perovskite solar cells with a ZnO/Zn₂SnO₄ composite compact layer. *Sol. Energ. Mater. Sol. Cells.* 2017;**159**:143-150

[35] Chang R, Yan Y, Zhang J, Zhu Z, Gu J. Large-grain and smooth cesium doped CH₃NH₃PbI₃ perovskite films by cesium iodide post-treatment for improved solar cells. *Thin Solid Films.* 2020;**712**:138279

[36] Chung I, Lee B, He J, Chang RPH, Kanatzidis MG. All-solid-state dye-sensitized solar cells with high efficiency. *Nature.* 2012;**485**:486-489

[37] Kumar MH, Dharani S, Leong WL, Boix PP, Prabhakar RR, Baikie T, et al. Lead-free halide perovskite solar cells with high photocurrents realized through vacancy modulation. *Advanced Materials.* 2014;**26**:7122-7127

[38] Noel NK, Stranks SD, Abate A, Wehrenfennig C, Guarnera S, Haghighirad A, et al. Environmental Science for photovoltaic applications. *Energy Environ Sci.* 2014;**7**:3061-3068

[39] Tai Q, Guo X, Tang G, You P, Ng TW, Shen D, et al. Antioxidant grain passivation for air-stable tin-based perovskite solar cells. *Angew. Chem. Int. Ed.* 2019;**58**:806-810

[40] Shao S, Liu J, Portale G, Fang HH, Blake GR, Brink GH, et al. Highly reproducible Sn-based hybrid perovskite solar cells with 9% efficiency. *Advanced Energy Materials.* 2018;**8**:1702019

[41] Bansode U, Naphade R, Game O, Agarkar S, Ogale S. Hybrid perovskite films by a new variant of pulsed excimer laser deposition: a room-temperature dry process. *Journal of Physical Chemistry C.* 2015;**119**:9177-9185

[42] Eperon GE, Eperon GE, Leijtens T, Bush KA, Prasanna R, Green T, et al. 2016. *Eperon.* 2016;**9717**:1-10

[43] Hao F, Stoumpos K, Cao DH, Chang RPH, Kanatzidis M. Lead-free solid state organic-inorganic halide perovskite solar cells. *Nature Photonics.* 2014;**8**:489-494

[44] Ramirez I, Zhang J, Ducati C, Grovenor C, Johnston MB, Ginger DS, et al. *Environmental science. Energy & Environmental Science.* 2016;**9**:2892-2901

[45] Lee S, Kang D. Highly efficient and stable Sn-rich perovskite solar cells by introducing bromine. *ACS Applied Materials & Interfaces.* 2017;**9**:22432-22439

[46] Jia H-L, Li S-S, Gong B-Q, Gu L, Bao Z-L, Guan M-Y. Efficient co sensitization of new organic dyes containing bipyridine anchors with porphyrins for dye-sensitized solar cells. *Sustainable Energy & Fuels.* 2020;**4**:347-353

[47] Fan Q, An Q, Lin Y, Xia Y, Li Q, Zhang M, et al. Over 14% efficiency all-polymer solar cells enabled by a low bandgap polymer acceptor with low energy loss and efficient charge separation. *Energy & Environmental Science.* 2020. DOI: 10.1039/D0EE01828G

[48] Dong X, Guo Q, Liu Q, Zhu L, Guo X, Liu F, et al. A naphthodithiophene-based nonfullerene acceptor for high-performance polymer solar cells with a small energy loss. *Journal of Materials Chemistry C.* 2020;**8**:6513-6520

[49] Ji K, Yuan J, Li F, Shi Y, Ling X, Zhang X, et al. High-efficiency perovskite quantum dot solar cells benefiting from a conjugated polymer-quantum dot bulk heterojunction connecting layer. *Journal of Materials Chemistry A*. 2020;8:8104-8112

[50] Rao H, Zhou M, Pan Z, Zhong X. Quantum dot material engineering boosting quantum dot sensitized solar cells efficiency over 13%. *Journal of Materials Chemistry A*. 2020;8:10233-10241

[51] Wen S, Li Y, Zheng N, Raji IO, Yang C, Bao X. High-efficiency organic solar cells enabled by halogenation of polymers based on 2D conjugated benzobis(thiazole). *Journal of Materials Chemistry A*. 2020;8:13671-13678